



Heriot-Watt University
Research Gateway

Pair-correlated stereodynamics for diatom-diatom rotational energy transfer: $\text{NO}(\text{A}^2\Sigma^+) + \text{N}_2$

Citation for published version:

Luxford, TFM, Sharples, TR, McKendrick, KG & Costen, ML 2017, 'Pair-correlated stereodynamics for diatom-diatom rotational energy transfer: $\text{NO}(\text{A}^2\Sigma^+) + \text{N}_2$ ', *The Journal of Chemical Physics*, vol. 147, no. 1, 013912. <https://doi.org/10.1063/1.4979487>

Digital Object Identifier (DOI):

[10.1063/1.4979487](https://doi.org/10.1063/1.4979487)

Link:

[Link to publication record in Heriot-Watt Research Portal](#)

Document Version:

Peer reviewed version

Published In:

The Journal of Chemical Physics

General rights

Copyright for the publications made accessible via Heriot-Watt Research Portal is retained by the author(s) and / or other copyright owners and it is a condition of accessing these publications that users recognise and abide by the legal requirements associated with these rights.

Take down policy

Heriot-Watt University has made every reasonable effort to ensure that the content in Heriot-Watt Research Portal complies with UK legislation. If you believe that the public display of this file breaches copyright please contact open.access@hw.ac.uk providing details, and we will remove access to the work immediately and investigate your claim.

Supplementary Material For

'Pair-correlated stereodynamics for diatom-diatom rotational energy transfer: NO(A²Σ⁺) + N₂'

Thomas F. M. Luxford,¹ Thomas R. Sharples,¹ Kenneth G. McKendrick¹ and Matthew. L. Costen^{1,a}

¹*Institute of Chemical Sciences, Heriot-Watt University, Edinburgh, EH14 4AS, United Kingdom*

I. Fitting to simulated data to determine sensitivity to basis image energy spacing

To determine the minimum energy spacing of basis images for fitting to the NO(A) + N₂ data, we first simulated experimental data, using the relevant experimentally determined molecular beam speeds for NO and N₂. We assumed that the N₂ was initially in rotational levels $j = 0$ and $j = 1$ only, and with ortho/para conservation constructed a simulation using the N₂ rotational transitions $j = 0$ to $j' = 0$ to 10 and $j = 1$ to $j' = 1$ to 9 in even- Δj steps. The differential cross sections (DCSs) for the simulation were taken from the previously published results of quantum scattering (QS) calculations for the NO(A) + He system.¹ These were chosen as they provide a series of DCSs that are structured and change from state-to-state in a consistent and physically plausible manner. For the $j \rightarrow j' = 0 \rightarrow 0$ and $1 \rightarrow 1$ transitions the DCS for $N = 0 \rightarrow N' = 3$ from the NO(A) + He QS calculations was used, and for the following transitions to final states $j' = 2$ to 10 the NO(A) + He QS DCSs for $N' = 4$ to 12 were used in sequence. The input DCSs are shown in Fig. S1 for each final N₂ rotational state. The simulation assumed that the angular momentum polarization was isotropic, i.e. that $A_{q+}^{(2)}(\theta) = 0$ for $q = 0$ and 2, for all scattering angles. As a result, the simulated V and H images were identical. The resulting single simulated image is shown in Fig. S2. We then fitted this simulated data with basis functions constructed using the available energies for the N₂ rotational transitions in Table I, and explored how many of these basis functions were required to accurately reproduce the simulated data. We used a Singular Value Decomposition (SVD) approach for the fitting, rather than the Simplex algorithm ultimately used to fit the experimental data. The SVD method is much faster than the Simplex, but has the disadvantage that physical constraints on the DCS (i.e. positive only) cannot be applied. If the basis functions used are insufficiently separate, the SVD fit will show this as correlations in the returned DCSs. Figure S1 shows the returned DCSs when basis functions for the $j = 0$ to $j' = 0, 4, 6, 8$ and 10 transitions were used, and Fig. S2 shows the resulting fit to the simulated data. The input DCS are returned in near quantitative agreement with the appropriate input DCS, with only the $j' = 6$ DCS showing significant disagreement, although even here the peak

^a Author to whom correspondence should be addressed. Electronic mail: m.l.costen@hw.ac.uk

scattering angle has been accurately identified. The introduction of more basis functions resulted in significant positive-negative correlations in adjacent DCSs, indicating over-determination of the fit. A further reduction in the number of basis functions reduced the agreement between simulation and fit, with residuals that indicated that the basis function spacing was now too sparse. We therefore concluded that under the conditions of the experiments reported here, the minimum energetic spacing of the basis functions was consistent with the $j = 0$ to $j' = 0, 4, 6, 8$ and 10 transitions only, where the smallest energy gap ($j' = 0$ to $j' = 4$) is 40 cm^{-1} .

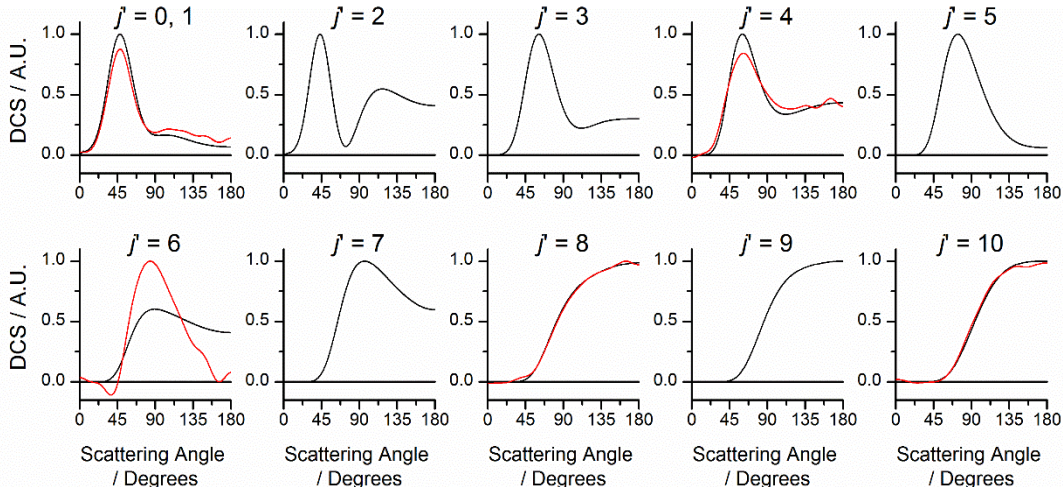


FIG S1. Black line: DCSs used to simulate the scattering image in Fig. S2 (from NO(A)-He QS calculations, at $\langle E_{col} \rangle = 670 \text{ cm}^{-1}$, $N' = 3-12$). Red line: DCSs fitted to the simulated image as described in the text.

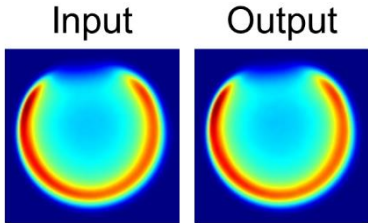


FIG S2. Left: Image simulated using the conditions of the NO(A)-N₂ experiment and the DCSs for the NO(A)-He scattering system shown in Fig. S1, with isotropic rotational alignment. Right: Image obtained from the results of fitting to the simulated image, returning the DCSs also shown in Fig. S1.

II. Determination of appropriate range of collider basis functions with experimental data

We explored the appropriate range of energies transferred to the unobserved collider, ΔE , to include in the full polarization dependent simplex fitting of the experimental data by performing SVD fits, assuming isotropic angular momentum polarization, with an increasing number of ΔE -dependent basis functions. We present the results of this procedure applied to a single NO(A) rotational state, $N' = 11$, in Fig. S3 and Fig. S4. Fig. S3(a) shows the experimental sum (V + H) image,

averaged over all 11 acquisitions. Fig. S3(b)-(d) show the fitted sum (V+H) images returned assuming: (a) three values of ΔE (0, 84 and 144 cm^{-1}), corresponding to $j = 0 \rightarrow j' = 0, 6$ and 8; (b) four values of ΔE (0, 84, 144 and 220 cm^{-1}), corresponding to $j = 0 \rightarrow j' = 0, 6, 8$ and 10; (c) four values of ΔE (0, 84, 144 and 312 cm^{-1}), corresponding to $j = 0 \rightarrow j' = 0, 6, 8$ and 12. In both Fig. S3(c) and Fig. S3(d) a faint ring corresponding to $j' = 10$ or 12 is visible, but which does not appear to visual inspection to be present in the experimental data. The overall residuals for the fits shown in Fig. S3(c) and Fig. S3(d) are not significantly smaller than that for the fit in Fig. S3(b), and in a visual inspection a systematic residual ring is observed for the highest N_2 energy.

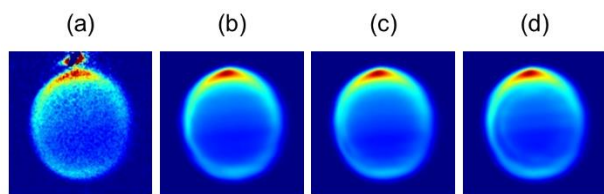


FIG S3. (a) Experimental NO(A)- N_2 V + H image, averaged across all acquisitions. Simulated images obtained from fitting the experimental image, using co-collider final rotational levels (b) $j' = 0, 6, 8$, (c) $j' = 0, 6, 8, 10$, (d) $j' = 0, 6, 8, 12$.

The returned DCSs for the fits shown in Fig. S3(b)-(d) are shown in Fig. S4(a)-(c). The amplitude of the returned DCSs for the high-energy $j' = 10$ and $j' = 12$ basis functions are small and the DCSs are near isotropic.

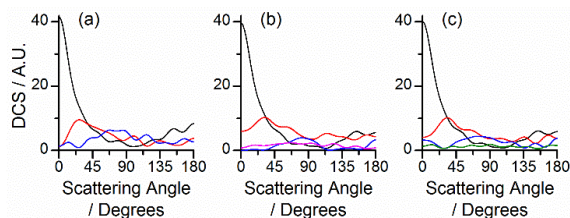


FIG S4. DCSs returned from the fits shown in Fig. S3, using co-collider final rotational levels (a) $j' = 0, 6, 8$, (b) $j' = 0, 6, 8, 10$, (c) $j' = 0, 6, 8, 12$. Black line: $j' = 0$, red line: $j' = 6$, blue line: $j' = 8$, magenta line: $j' = 10$, green line: $j' = 12$.

The combination of the small amplitude, isotropic DCS and the behavior of the residuals led us to conclude that there was little or no amplitude of these basis functions in the experimental data, and that what was returned was primarily the result of fitting to high-frequency noise across the center of the image. We accordingly decided to truncate the energy expansion at three basis functions, corresponding to $j = 0 \rightarrow j' = 0, 6$ and 8 ($\Delta E = 0, 84$ and 144 cm^{-1}).

III. Effect of Angular Momentum Polarization on the Fitted DCSs.

In principle, there could be a correlation between the returned DCSs and the rotational angular momentum moments, for example the $A_{2+}^{\{2\}}(\theta)$ moment for $j' = 0$ and the DCS for $j' = 8$ are both determined by the intensities of pixels across the interior of the image, although with different dependences on the probe polarization. We tested the influence of the angular momentum polarization on the returned DCSs by fitting the experimental images with an assumption of isotropic angular momentum polarization, i.e. $A_{q+}^{\{2\}}(\theta) = 0$ for $q = 0$ and 2 for all scattering angles. The DCSs resulting from this fit for the $N' = 6, 8$ and 11 states are compared to the DCSs resulting from the full, polarization-dependent, fit in Fig. S5. The results are indistinguishable for all N' -states and j' -energies. This confirms that the DCSs returned are independent of the alignment moments, and illustrates the remarkable degree of separation of the dependence of the experimental images to the DCS and alignment moments previously reported for the results of NO(A) + Rg scattering in our apparatus.¹⁻³

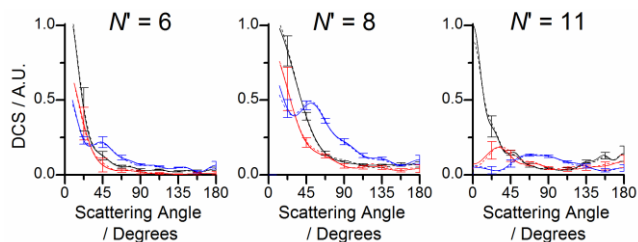


FIG. S5. Differential cross sections for the collisions of NO(A) with N_2 at $\langle E_{col} \rangle = 797 \text{ cm}^{-1}$, for final NO(A) rotational levels $N' = 3, 8$ and 11, obtained with assumed isotropic rotational alignment (solid lines) and simultaneously fit rotational alignment (dashed). Different plots on the same axis represent the different final N_2 rotational levels: black: $j' = 0$, red: $j' = 6$, blue: $j' = 8$. Error bars represent 95% confidence limits of the DCSs fitted to the images with isotropic rotational alignment.

References

1. T. F. M. Luxford, T. R. Sharples, D. Townsend, K. G. McKendrick, and M. L. Costen, *J Chem Phys* **145**, 084312 (2016).
2. T. F. M. Luxford, T. R. Sharples, K. G. McKendrick, and M. L. Costen, *J Chem Phys* **145**, 174304 (2016).
3. T. R. Sharples, T. F. M. Luxford, D. Townsend, K. G. McKendrick, and M. L. Costen, *J Chem Phys* **143**, 204301 (2015).